

# Accelerated Brain Aging in Schizophrenia and Beyond: A Neuroanatomical Marker of Psychiatric Disorders

Nikolaos Koutsouleris<sup>\*1</sup>, Christos Davatzikos<sup>2</sup>, Stefan Borgwardt<sup>3</sup>, Christian Gaser<sup>4</sup>, Ronald Bottlender<sup>1</sup>, Thomas Frodl<sup>1</sup>, Peter Falkai<sup>1</sup>, Anita Riecher-Rössler<sup>3</sup>, Hans-Jürgen Möller<sup>1</sup>, Maximilian Reiser<sup>5</sup>, Christos Pantelis<sup>6</sup>, and Eva Meisenzahl<sup>1</sup>

<sup>1</sup>Department of Psychiatry and Psychotherapy, Ludwig-Maximilian University, Munich, Germany; <sup>2</sup>Center for Biomedical Image Computing and Analytics, University of Pennsylvania, Philadelphia, PA; <sup>3</sup>Department of Psychiatry, University of Basel, Basel, Switzerland; <sup>4</sup>Structural Brain Imaging Group, Department of Psychiatry and Neurology, Friedrich Schiller University, Jena, Germany; <sup>5</sup>Department of Radiology, Ludwig-Maximilian University, Munich, Germany; <sup>6</sup>Melbourne Neuropsychiatry Center, University of Melbourne, Melbourne, Victoria, Australia

\*To whom correspondence should be addressed; Department of Psychiatry and Psychotherapy, Ludwig-Maximilian University, Nussbaumstr. 7, 80336 Munich, Germany; tel: 49-(89)-5160-5717, fax: 49-(89)-5160-4749, e-mail: [nikolaos.koutsouleris@med.uni-muenchen.de](mailto:nikolaos.koutsouleris@med.uni-muenchen.de)

**Structural brain abnormalities are central to schizophrenia (SZ), but it remains unknown whether they are linked to dysmaturational processes crossing diagnostic boundaries, aggravating across disease stages, and driving the neurodiagnostic signature of the illness. Therefore, we investigated whether patients with SZ ( $N = 141$ ), major depression (MD;  $N = 104$ ), borderline personality disorder (BPD;  $N = 57$ ), and individuals in at-risk mental states for psychosis (ARMS;  $N = 89$ ) deviated from the trajectory of normal brain maturation. This deviation was measured as difference between chronological and the neuroanatomical age (brain age gap estimation [BrainAGE]). Neuroanatomical age was determined by a machine learning system trained to individually estimate age from the structural magnetic resonance imagings of 800 healthy controls. Group-level analyses showed that BrainAGE was highest in SZ (+5.5 y) group, followed by MD (+4.0), BPD (+3.1), and the ARMS (+1.7) groups. Earlier disease onset in MD and BPD groups correlated with more pronounced BrainAGE, reaching effect sizes of the SZ group. Second, BrainAGE increased across at-risk, recent onset, and recurrent states of SZ. Finally, BrainAGE predicted both patient status as well as negative and disorganized symptoms. These findings suggest that an individually quantifiable “accelerated aging” effect may particularly impact on the neuroanatomical signature of SZ but may extend also to other mental disorders.**

*Key words:* neuroanatomical dysmaturation/biomarker/machine learning/accelerated aging/schizophrenia/depression/borderline personality disorder

## Introduction

From adolescence to adulthood, the brain’s neural architecture is profoundly remodeled, involving synaptic elimination, dendritic pruning, and myelination.<sup>1</sup> At the macroscopic level, significant gray matter (GM) reductions within the prefronto-temporo-limbic cortices may reflect this maturational process, which shapes the substrate of complex and integrated behavior in adult life. Importantly, these age-related changes seem to be so well conserved across individuals that they constitute a tightly controlled intermediate phenotype of normal brain maturation,<sup>2</sup> which enables the single-subject quantification of abnormal age-related neurodevelopment by using magnetic resonance imaging (MRI)-based multivariate pattern analysis (MVPA).<sup>2-4</sup>

Intriguingly, the transition from adolescence to adulthood does not only host the normal maturation of neural circuitry, but it is also associated with the highest incidence rates of psychoses. These observations inspired the “two-hit” hypothesis of schizophrenia (SZ),<sup>5</sup> postulating that a “late” neurodevelopmental process is disturbed in this vulnerable phase due to an early neurobiological “hit” in the pre- and perinatal period. This theory assumes that higher order cortical systems involving prefrontal, temporal, and limbic structures are susceptible to deviations from their maturational trajectories.<sup>1,6,7</sup> These deviations may lead to brain alterations that accumulate across subsequent disease stages<sup>8,9</sup> and, thus, may point to a process of “accelerated aging” in SZ.<sup>10,11</sup>

This hypothesis requires thorough evaluation by contrasting disease-specific findings with changes in the normally maturing brain.<sup>12</sup> Furthermore, because considerable neuroanatomical overlaps have been found between nonaffective and affective psychoses,<sup>13</sup> it remains unclear if maturational processes may only be altered in SZ or across nosological boundaries. Finally, previous MRI studies revealed high diagnostic classification rates (70%–90%) of patients with schizophrenic or affective psychoses vs healthy controls (HCs).<sup>14</sup> It is unknown whether the diagnostic signatures underlying these results emerge from an altered neurodevelopment in SZ and beyond. This question is of crucial relevance for future imaging-based diagnostic tools in psychiatry because disease-specific deviations from the normal maturational trajectories may evolve dynamically, thus determining the diagnostic performance of MRI-based biomarkers across the life span.<sup>15</sup>

To investigate these questions, we first constructed a multivariate model of neuroanatomical brain maturation enabling the single-subject estimation of age in a large MRI database of HCs. Then, this age predictor was applied to a transnosological database of different diagnostic groups that include patients with SZ, major depression (MD), borderline personality disorder (BPD), and individuals in at-risk mental states (ARMS) for psychosis in order to quantify their deviations from the normal maturational trajectory using brain age gap estimation (BrainAGE).<sup>4</sup> Furthermore, BrainAGE was used to compare disease stages of SZ, consisting of early and late ARMS (ARMS-E and ARMS-L, respectively), recent-onset (RO), and recurrently ill (RE) SZ patients. Moreover, we assessed whether BrainAGE determined a separately trained MVPA classifier's ability to individually separate SZ, MD, and BPD patients from HCs. Finally, we examined the impact of sociodemographic and clinical variables on BrainAGE variation in SZ patients and HCs. We expected to find (1) BrainAGE increments predominantly in SZ group compared with MD and BPD groups, in line with the “accelerated aging” hypothesis of SZ,<sup>10,11</sup> and (2) an increasing BrainAGE gradient from ARMS through RE-SZ individuals. We hypothesized that BrainAGE predicts the single-subject separability of SZ, MD, and BPD patients vs HCs due to a considerable overlap of age- and disease-related brain variation.

## Methods

### Study Participants

A structural MRI database of 800 HCs, aged 18–65 and recruited across 5 centers, was created in order to train the multivariate age predictor (definitions are given in [table 1](#)). Patients were enrolled at the Department of Psychiatry and Psychotherapy, Ludwig-Maximilian University, Munich ([tables 1 and 3](#)). Patient evaluations

included the Structured Clinical Interview for Diagnostic and Statistical Manual of Mental Disorders, Fourth Edition (DSM-IV): Axis I and II Disorders, the review of records and psychotropic medications ([table 3](#)) as well as symptom assessments using the Positive and Negative Symptom Scale (PANSS)<sup>21</sup> in SZ and BPD groups, the Scale for the Assessment of Negative Symptoms<sup>22</sup> in SZ group, and the Hamilton Depression Rating Scale<sup>23</sup> in MD and BPD groups. A consensus diagnosis was achieved by two experienced psychiatrists at study inclusion and after 1 year using the DSM-IV. Doses of antipsychotic medications at MRI were converted to chlorpromazine equivalents.<sup>24</sup>

Additionally, a sample of 89 ARMS individuals was generated by pooling the Munich ( $N = 52$ ) and *Früherkennung von Psychosen (FePsy)*<sup>25</sup> ( $N = 37$ ) databases. In both databases, an ARMS-L for psychosis was defined by established operationalized ultra-high-risk criteria ([table 1](#)). The Munich sample also included individuals with ARMS-E ([table 1](#)). Seventy-two ARMS individuals were regularly followed over 4–7 years to detect a disease transition, as defined by psychotic symptoms occurring daily and persisting for more than 1 week.<sup>19</sup> Transition to SZ ( $N = 29$ ) or schizoaffective psychosis ( $N = 4$ ) occurred in 33 individuals. Diagnoses were confirmed by DSM-IV criteria 1 year after transition. Only 4 ARMS subjects received atypical antipsychotics (3 olanzapine and 1 risperidone) for less than 3 weeks prior to MRI scanning. Symptom severity was measured using the PANSS in the Munich sample and Brief Psychiatric Rating Scale in the *FePsy* sample.

SZ patients with an illness duration of <1 year, no previous inpatient treatment, and <12 months (lifetime) of antipsychotic treatment were assigned to the RO-SZ subgroup or to the RE-SZ sample if not fulfilling these criteria. Illness duration was the time interval between MRI scanning and disease onset defined retrospectively by the onset of symptoms paralleled by a general decline in social and role functioning.<sup>26</sup> All participants gave their written informed consent prior to study inclusion. The study design was approved by the local ethics committee and was prepared in accordance with the ethical standards of the Declaration of Helsinki.

### MRI Data Acquisition and Preprocessing

All MR images were processed using the VBM8 toolbox<sup>27</sup> and SPM8 software, which generated GM maps in the original MRI space of each participant ([table 2](#); [online supplementary methods 1](#)).<sup>28</sup> Then, a dual registration strategy captured both large-scale and focal neuroanatomical variation in the study population: first, the GM maps were affinely registered to the single-subject Montreal Neurological Institute template, thus removing global brain volume differences across subjects

**Table 1.** Exclusion/Inclusion Criteria for Each Study Group in the Multicenter Database

Center	<i>N</i>	Mean Age ( <i>SD</i> )	Exclusion Criteria
(A) 800 HCs used for training and cross-validation of the multivariate age predictor Munich database: Department of Psychiatry and Psychotherapy, Ludwig-Maximilian University, Munich	288	36.8 (11.1)	(1) Age <18 or >65, (2) positive medical history for head trauma with loss of consciousness, (3) cortisol treatments, (4) any somatic conditions affecting the central nervous system, (5) present or past abuse of alcohol or other drugs, and (6) a personal or familial history of psychiatric disorders (first-degree relatives)
IXI database: (1) Hammersmith Hospital, Imperial College, London	99	39.8 (15.5)	(1) Age <18 or >65, (2) acute somatic, and/or (3) current psychiatric conditions <sup>a</sup>
(2) Institute of Psychiatry, King's College, London	60	39.1 (13.7)	
(3) Guy's Hospital, NHS Foundation Trust, London	137	38.5 (12.1)	
OASIS database: Washington University	216	38.9 (18.0)	(1) Age <18 or >65, (2) present or past psychiatric or neurological diagnosis, (3) present or past medical conditions (eg, stroke, serious head injury) affecting the central nervous system, (4) history of psychoactive drug use, and (5) gross MRI abnormalities <sup>16</sup>
Center	<i>N</i>	Mean Age ( <i>SD</i> )	Inclusion/Exclusion Criteria
(B) Data used for validation and patient evaluation Munich database: groups with 127 HCs, 141 SZ, 104 MD, 57 BPD, and 52 ARMS	481	HC: 24.9 (3.7) ARMS: 24.9 (5.5)  Other groups: see <a href="#">table 2</a>	(1) Inclusion criteria: Patient groups: respective DSM-IV diagnostic criteria ARMS-E: predictive basic symptoms <sup>17</sup> and/or risk-conferring global functioning and trait criteria <sup>18</sup> ARMS-L: attenuated psychotic symptoms and/or brief limited intermittent psychotic symptoms that closely correspond to the ultrahigh-risk definitions of the PACE clinic in Melbourne <sup>19</sup> (2) Exclusion criteria: General: current or past psychiatric comorbidities, including (1) mental retardation, (2) anorexia nervosa, (3) delirium, (4) dementia or (5) amnesic disorders, and (6) substance dependence and/or somatic conditions affecting the central nervous system HC: see Munich database definitions in (A) SZ: mood and personality disorders MD: SZ spectrum and personality disorders BPD: bipolar and SZ spectrum disorders ARMS: current or past diagnoses of SZ spectrum, bipolar and personality disorders or psychosis transition criteria <sup>19</sup>

**Table 1.** (Continued)

Center	<i>N</i>	Mean Age ( <i>SD</i> )	Exclusion Criteria
Basel <i>FePsy</i> study: groups with 22 HCs and 37 ARMS	59	HC: 23 (4.3) ARMS: 24.8 (6.3)	HC: see HC exclusion criteria in Borgwardt et al <sup>20</sup> ARMS: criteria that closely correspond to the PACE criteria and to the definitions applied in the Munich database (ARMS-L inclusion criteria as well as general and ARMS-specific exclusion criteria) <sup>20</sup>

*Note:* ARMS-E, early at-risk mental states; ARMS-L, late at-risk mental states; BPD, borderline disorder; DSM-IV, Diagnostic and Statistical Manual of Mental Disorders, Fourth Edition; *FePsy*, Früherkennung von *Psychosen*; HC, healthy control; IXI, Information eXtraction from Images; MD, major depression; MRI, magnetic resonance imaging; NHS, National Health Service; OASIS, Open Access of Imaging Studies; PACE, Personal Assessment and Crisis Evaluation; SZ, schizophrenia.

<sup>a</sup>Personal communication by Prof. D. Rueckert, Imperial College London.

**Table 2.** MRI Scanners and Data Acquisition Protocols Used in the Study

Center	MRI Scanner	MRI Acquisition Parameters
Munich database	Siemens MAGNETOM Vision 1.5T	TR: 11.6 ms; TE: 4.9 ms; 126 contiguous slices of 1.5-mm thickness; matrix: 512 × 512; voxel size: 0.45 × 0.45 × 1.5 mm; field of view: 230 mm
IXI database, Hammersmith Hospital	Philips Intera 3.0T	TR: 9.6 ms; TE: 4.6 ms; phase encoding steps: 208; echo train length: 208; reconstruction diameter: 240 mm; matrix: 208 × 208; flip angle: 8°
IXI database, Institute of Psychiatry IXI database, Guy's Hospital	Philips Gyroscan Intera 1.5T General Electric 1.5T	NA TR: 9.8 ms; TE: 4.6 ms; phase encoding steps: 192; echo train length: 0; reconstruction diameter: 240 mm; flip angle: 8°
OASIS database	Siemens MAGNETOM Vision 1.5T	TR: 9.7 ms; TE: 4.0 ms; 128 contiguous slices of 1.25-mm thickness; matrix: 256 × 256; voxel size: 1.0 × 1.0 × 1.25 mm; flip angle: 8°
Basel <i>FePsy</i> study	Siemens MAGNETOM Vision 1.5T	TR: 9.7 ms; TE: 4 ms; 176 contiguous slices of 1-mm thickness; matrix: 200 × 256; voxel size: 1.28 × 1 × 1 mm; field of view: 25.6 × 25.6 cm; flip angle: 12°

*Note:* NA, not available; TE, time-to-echo; TR, relaxation time. Abbreviations are explained in the first footnote to [table 1](#).

while retaining large-scale, interindividual morphometric variation. Second, these maps were high dimensionally registered to the template using the DRAMMS algorithm,<sup>29</sup> which encoded focal, nonlinear tissue deformations in each individual brain relative to the template. The resulting deformations and warped tissue maps were used to compute GM maps allowing for a Regional Analysis of brain Volumes in Normalized Space (GM-RAVENS).<sup>30</sup>

#### Support Vector Regression for MRI-Based Age Prediction

Across diverse biomedical fields, support vector machines (SVM) demonstrated their ability to learn multivariate prediction rules that generalize well across study populations, thus enabling individualized diagnostic classification and function approximation (online [supplementary](#)

[methods 2](#)).<sup>31</sup> We used linear v-support vector regression (v-SVR)<sup>32</sup> to predict age from each subject's MRI by constructing predictive models from one set of subjects (the training sample) and applying them to a different set of subjects (the test sample), using cross-validation (CV).<sup>33,34</sup> This produced a completely unbiased estimate of the method's age prediction performance in new individuals, rather than merely fitting the current study population. More specifically, our prediction pipeline was wrapped into a repeated nested CV framework consisting of 10 repetitions × 10 ms folds at the outer and inner CV cycles, as detailed previously.<sup>33,34</sup> Each training sample at the inner CV loop was processed as follows: first, the multivariate RGS (Regression, Gradient guided Feature selection) algorithm<sup>35,36</sup> ranked voxels in the GM-RAVENS and affine maps according to their age prediction relevance. Each GM input space was scaled using the respective weight vectors and projected to 400 predictive

**Table 3.** Sociodemographic and Clinical Data

Variables	Groups in Analysis 1					Groups in Analysis 2								
	HC <sub>1</sub>	SZ	MD	BPD	ARMS	F <sub>1</sub> χ <sup>2</sup>	P	HC <sub>2</sub>	ARMS-E	ARMS-L	RO-SZ	RE-SZ	F <sub>1</sub> χ <sup>2</sup>	P
<b>Sociodemographic data</b>														
N	437	141	104	57	89	—	—	102	21	68	61	80	—	—
Age (y), mean (SD)	32.6 (10.9)	28.5 (7.32)	42.3 (12.0)	25.6 (6.7)	24.9 (5.8)	50.9	<.001	26.5 (5.9)	25.6 (5.6)	24.6 (5.9)	26.3 (5.8)	30.3 (7.9)	8.0	<.001
Sex, M/F (% M)	223/214 (51.0%)	108/33 (76.6%)	52/52 (50%)	0/57 (0%)	56/33 (62.9%)	100.4	<.001	73/29 (71.6%)	10/11 (47.6%)	46/22 (67.6%)	45/16 (73.8%)	63/17 (78.8%)	8.6	.072
Handedness, R/L/Ambi. (%R)	371/45/9 (87.2%)	130/8/3 (92.2%)	74/4/0 (94.9%)	53/4/0 (93.0%)	78/8/3 (87.6%)	9.0	.335	79/17/2 (80.6%)	17/3/1 (81%)	61/5/2 (89.7%)	55/5/1 (90.2%)	75/3/2 (93.8%)	11.3	.179
Body mass index, mean (SD) <sup>a</sup>	23.3 (3.3)	24.1 (4.4)	23.9 (4.1)	24.2 (5.0)	22.1 (3.0)	3.3	.011	22.7 (3.1)	21.1 (2.4)	23.0 (3.3)	23.0 (4.4)	24.9 (4.2)	5.5	<.001
Schooling (y), mean (SD)	12.2 (1.3)	10.7 (2.0)	10.8 (1.7)	11.2 (1.6)	11.2 (1.9)	31.5	<.001	12.0 (1.2)	11.5 (2.9)	11.1 (1.5)	10.8 (2.1)	10.6 (1.8)	9.1	<.001
Alcohol (g/day), mean (SD) <sup>a</sup>	8.0 (10.3)	11.2 (25.5)	11.2 (21.1)	8.1 (24.5)	5.7 (12.4)	1.8	.128	9.6 (13.5)	2.9 (5.6)	7.7 (15.3)	11.7 (20.2)	10.8 (29.1)	0.8	.525
Nicotine (no. of cigarettes/day), mean (SD) <sup>a</sup>	3.9 (7.5)	13.2 (13.7)	9.7 (13.4)	10.5 (11.5)	7.0 (9.8)	24.0	<.001	3.6 (7.3)	7.0 (9.9)	7.0 (9.8)	13.8 (14.6)	12.7 (13.0)	8.6	<.001
<b>Clinical data</b>														
Age of onset (y), mean (SD)	—	24.2 (6.2)	36.5 (12.0)	16.5 (5.9)	—	101.3	<.001	—	—	—	26.1 (5.8)	22.7 (5.7)	11.7	.001
Illness duration (y), mean (SD)	—	4.3 (6.4)	5.8 (7.8)	9.4 (7.5)	—	8.7	<.001	—	—	—	0.29 (0.20)	7.2 (7.1)	57.1	<.001
AP at MRI, no. of patients (%)	—	126 (90.0%)	18 (17.3%)	20 (38.5%)	—	135.0	<.001	—	—	—	49 (81.7%)	77 (96.2%)	8.1	.008
Typical AP at MRI, no. of patients (%)	—	45 (32.1%)	10 (9.6%)	9 (17.3%)	—	18.6	<.001	—	—	—	21 (35.0%)	24 (30.0%)	0.4	.585
Atypical AP at MRI, no. of patients (%)	—	95 (67.9%)	9 (8.7%)	12 (23.1%)	—	94.6	<.001	—	—	—	33 (55.0%)	62 (77.5%)	8.0	.006
Typical and atypical AP at MRI, no. of patients (%)	—	14 (10.0%)	1 (1.0%)	1 (1.9%)	—	11.0	.005	—	—	—	5 (8.3%)	9 (11.2%)	0.3	.777
CPZ-equivalent dose (mg), mean (SD)	—	358.9 (382.4)	43.8 (162.0)	91.1 (266.8)	—	35.2	<.001	—	—	—	303.2 (392.2)	404.4 (370.7)	1.6	.212
Antidepressants at MRI, no. of patients (%) <sup>a</sup>	—	11 (7.9%)	76 (73.1%)	38 (66.7%)	9 (17.3%)	134.6	<.001	—	5 (23.8%)	4 (12.9%)	1 (1.6%)	10 (12.7%)	10.3	.015
Mood stabilizers at MRI, no. of patients (%)	—	5 (3.6%)	13 (12.5%)	11 (21.2%)	—	14.7	.006	—	—	—	0 (0%)	5 (6.3%)	4.0	.068

Table 3. (Continued)

Variables	Groups in Analysis 1						Groups in Analysis 2							
	HC <sub>1</sub>	SZ	MD	BPD	ARMS	F/ $\chi^2$	P	HC <sub>2</sub>	ARMS-E	ARMS-L	RO-SZ	RE-SZ	F/ $\chi^2$	P
Lithium at MRI, no. of patients (%)	—	0 (0%)	7 (6.7%)	1 (1.9%)	—	—	10.4	<b>.006</b>	—	—	0 (0%)	0 (0%)	—	—
PANSS total, mean (SD) <sup>a</sup>	—	81.9 (28.9)	—	70.0 (18.4)	60.1 (19.6)	12.2	<b>&lt;.001</b>	—	56.8 (14.0)	62.0 (22.2)	77.6 (32.8)	85.1 (25.4)	7.4	<b>&lt;.001</b>
PANSS positive, mean (SD) <sup>a</sup>	—	18.3 (8.0)	—	12.8 (5.1)	12.3 (4.3)	17.7	<b>&lt;.001</b>	—	9.86 (2.6)	13.7 (4.5)	19.7 (8.2)	17.2 (7.7)	8.8	<b>&lt;.001</b>
PANSS negative, mean (SD) <sup>a</sup>	—	22.2 (9.6)	—	13.8 (5.0)	15.4 (7.8)	20.8	<b>&lt;.001</b>	—	14.9 (6.7)	15.7 (8.5)	19.4 (10.1)	24.4 (8.7)	9.1	<b>&lt;.001</b>
PANSS general, mean (SD) <sup>a</sup>	—	41.4 (16.0)	—	43.4 (10.7)	32.4 (10.0)	7.5	<b>.001</b>	—	32.0 (7.9)	32.6 (11.1)	38.6 (18.2)	43.5 (13.8)	4.9	<b>.003</b>
SANS sum, mean (SD)	—	44.7 (26.9)	—	—	—	—	—	—	—	—	37.5 (28.8)	49.8 (24.5)	3.6	<b>.031</b>
HAMD sum, mean (SD)	—	—	21.3 (9.5)	22.4 (11.5)	—	0.26	.614	—	—	—	—	—	—	—

Note: Ambi., ambidextrous; AP, antipsychotic; CPZ, chlorpromazine; HAMD, Hamilton Depression Rating Scale; L, left; PANSS, Positive and Negative Symptom Scale; R, right; RE, recurrently ill; RO, recent onset; SANS, Scale for the Assessment of Negative Symptoms. Abbreviations are explained in the first footnote to table 1. The HC<sub>1</sub>, HC<sub>2</sub>, and ARMS groups include subjects from the Munich and FePsy databases. Statistics: F test value of ANOVA;  $\chi^2$ : value of chi-square test. Bold values are significant at  $P < 0.05$ .  
<sup>a</sup>Analysis includes only Munich ARMS data ( $N = 52$ ) because FePsy information was unavailable.

eigenvariates<sup>4</sup> using principal component analysis (PCA).<sup>18</sup> Finally, the v-SVR generated a linear kernel projection from the training cases' eigenvariate loadings and determined an optimal age-fitting function in kernel space. Fitting was controlled by the v-SVR's parameters, which were optimized in the inner CV cycle.

Each test person's age was estimated by applying the trained prediction system (RGS, PCA, and v-SVR models) to the respective test data. Age estimations were averaged across those models, for which the test person had not been involved in the training process. This out-of-training prediction performance was quantified using the mean absolute error (MAE) and explained variance ( $R^2$ ). Individual errors were measured using BrainAGE.<sup>4</sup> Finally, the trained predictor was applied to the 302 patients (SZ, MD, and BPD) and the 89 ARMS individuals to obtain BrainAGE scores. Additionally, we evaluated whether an age prediction system trained only in the Munich HC database would considerably change the results of our analyses (online supplementary analysis 3).

#### BrainAGE analyses

Sociodemographic, clinical, and BrainAGE group-level differences were assessed across HC<sub>1</sub>, SZ, MD, BPD, and ARMS samples (analysis 1) and HC<sub>2</sub>, ARMS-E, ARMS-L, RO-SZ, and RE-SZ groups (analysis 2) (table 3; figure 1). Continuous variables were evaluated using ANOVAs, and categorical variables were evaluated using  $\chi^2$  tests. Significance was defined at  $P < .05$ .

For the patient groups in analysis 1, we further assessed main BrainAGE effects of diagnosis, age of disease onset, and illness duration as well as the predictor  $\times$  group interactions using ANCOVA. In analysis 2, we additionally evaluated main BrainAGE and interaction effects of disease stage (RO-SZ vs RE-SZ), age of onset, and symptom severity (PANSS total). Furthermore, effects of sociodemographic and clinical variables on BrainAGE were explored in the ARMS, patient (table 4), and HC groups (online supplementary analysis 1). Finally, we assessed whether a multivariate set of 62 clinical variables allowed for the single-subject prediction of BrainAGE in 125 SZ patients using v-SVR regression (online supplementary analysis 2).

#### Single-Subject Patient Separability and Individual BrainAGE Scores

To evaluate the influence of BrainAGE on MRI-based patient classification, we trained a v-SVM classifier (v-SVC) to distinguish between 302 patients (SZ, MD, and BPD) and 302 age- and sex-matched HCs from the Munich database. As previously described, we entered both GM-RAVENS and affine GM maps into a 3-step machine learning pipeline, consisting of multivariate voxel weighting, PCA, and v-SVC. Again, all

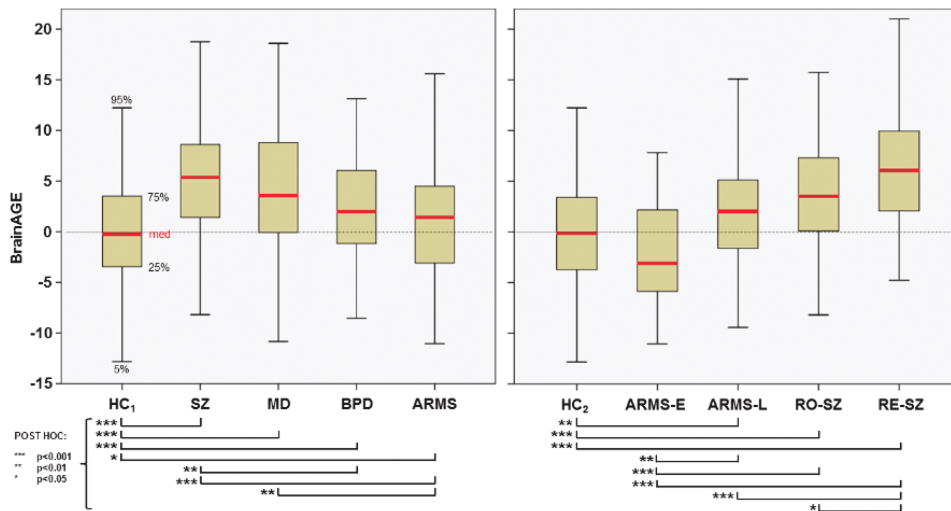


**Fig. 1.** Group-level brain age gap estimation (BrainAGE) analyses. Box plots of BrainAGE distributions across study groups in analyses 1 and 2 and respective pairwise post hoc comparisons.

computations were wrapped into repeated, nested CV, as described above.<sup>20,33,34</sup> The SVM’s  $\nu$  hyperparameter was a priori set to 0.5.

The trained classifier was applied to the test cases resulting in group predictions and decision values measuring the distance between the respective subject and the SVM’s decision boundary. The out-of-training classifier performance was quantified as accuracy and area under the curve (AUC) (figure 2). Correlations between patient separability (decision values) and BrainAGE as well as overlaps between patient- and age-predictive patterns were shown in figure 2.

**Results**

*Sociodemographic and Clinical Parameters*

The HC<sub>1</sub>, patient (SZ, MD, and BPD), and ARMS groups differed regarding age, sex, education, and nicotine consumption (table 3). Illness onsets and durations varied significantly between patient groups: BPD group started earliest and showed longer duration compared with SZ ( $P < .001$ ) and MD ( $P = .006$ ) groups. The MD group was characterized by the latest onset: mean (SD): 36.5 (12.0) years, whereas SZ commenced at mean (SD): 24.2 (6.2) years. As expected, antipsychotic medication at MRI was more prevalent in SZ (90%) vs MD, BPD, and ARMS groups, whereas antidepressants were more prevalent in MD (73.1%) vs the other groups (table 3). Mood stabilizer prescription was low, with BPD group showing the highest prescription rate (21.6%; table 3).

HC<sub>2</sub>, ARMS-E, ARMS-L, RO-SZ, and RE-SZ groups differed regarding age, schooling years, body mass index, and nicotine consumption (table 3). PANSS total score was significantly higher in RE-SZ vs ARMS-E and ARMS-L ( $P < .001$ ) groups, with the PANSS negative subscore in RE-SZ exceeding all other samples (table 3).

RE-SZ patients were more frequently treated with antipsychotics in general, atypical antipsychotics, and antidepressants compared with RO-SZ patients.

*Individualized Age Prediction in HCs*

The  $\nu$ -SVR predictor estimated age with a MAE of 4.6 years ( $R^2 = .83$ ;  $T = 62.7$ ;  $P < .001$ ) in single out-of-training HCs (figure 3). Age-predictive brain regions are shown in figure 4.

*BrainAGE Across Diagnoses*

BrainAGE differed across groups (figure 1;  $F = 29.2$ ;  $P < .001$ ), with the SZ group showing the most pronounced BrainAGE increase vs HCs (mean [SD]: +5.5 [6.0] y), followed by MD (+4.0 [6.2]), BPD (+3.1 [6.8]), and ARMS (+1.7 [7.2]) groups. Between-group differences were found in SZ vs BPD ( $P < .007$ ) group, SZ vs ARMS ( $P < .001$ ) group, and MD vs ARMS ( $P < .005$ ) group.

Furthermore, we detected an independent main BrainAGE effect of age of disease onset ( $F = 11.2$ ;  $P < .001$ ) across diagnoses but detected no effects of diagnosis, illness duration, or diagnosis  $\times$  clinical predictor interactions. Post hoc regression analyses showed that MD ( $r = -.34$ ,  $T = -3.23$ ;  $P < .002$ ) and BPD groups ( $r = -.42$ ,  $T = -2.58$ ;  $P < .014$ ), but not the SZ group ( $r = -.07$ ,  $T = -0.79$ ;  $P < .432$ ), were driving age of onset effects based on negative BrainAGE correlations. We further explored these effects by median-splitting samples and defining “early vs late onset” as factor in an additional ANCOVA. Again, main effects of this factor survived after controlling for diagnosis and illness duration (BrainAGE marginal means [SD] in early- vs late-onset patients: +5.9 [0.7] vs +3.1 [0.6];  $F = 10.1$ ;  $P = .002$ ). No independent main effect of diagnosis was found (SZ =

**Table 4.** Exploratory Association Analyses Between BrainAGE and Sociodemographic and Clinical Variables

Association Between BrainAGE and ...	Groups in Analysis 1					Groups in Analysis 2				
	HC <sub>1</sub>	SZ	MD	BPD	ARMS	HC <sub>2</sub>	ARMS-E	ARMS-L	RO-SZ	RE-SZ
(i) Sociodemographic variables										
Educational years, <i>R</i> ( <i>P</i> )	.004 (.930)	-.150 (.079)	-.074 (.527)	-.010 (.950)	.025 (.815)	-.028 (.787)	.262 (.252)	-.079 (.524)	-.243 (.063)	-.002 (.985)
Body mass index, <i>R</i> ( <i>P</i> )	.071 (.178)	.157 (.066)	-.012 (.917)	.133 (.406)	.078 (.626)	.156 (.188)	-.425 (.079)	.287 (.184)	<b>.364 (.005)</b>	-.068 (.559)
(ii) Nicotine and alcohol use (cigarettes/day), <i>R</i> ( <i>P</i> )	-.049 (.345)	.018 (.832)	-.063 (.537)	.198 (.241)	.151 (.306)	<b>-.273 (.023)</b>	.140 (.555)	.164 (.405)	.145 (.277)	-.057 (.623)
Alcohol (g/day), <i>R</i> ( <i>P</i> )	.047 (.365)	.078 (.369)	.012 (.905)	-.004 (.983)	.074 (.616)	.095 (.438)	-.171 (.471)	.110 (.577)	-.090 (.500)	.162 (.161)
(iii) Disease course data										
Age of onset (y), <i>R</i> ( <i>P</i> )	—	-.084 (.322)	<b>-.261 (.007)</b>	<b>-.338 (.026)</b>	—	—	—	—	-.097 (.458)	.013 (.911)
Illness duration (y), <i>R</i> ( <i>P</i> )	—	.042 (.619)	-.125 (.205)	.073 (.644)	—	—	—	—	-.149 (.253)	-.084 (.464)
(iv) Psychotropic medication										
CPZ equivalents, <i>R</i> ( <i>P</i> )	—	.023 (.799)	-.128 (.202)	.183 (.229)	—	—	—	—	.014 (.916)	-.024 (.843)
Antipsychotic use (yes/no), <i>F</i> ( <i>P</i> )	—	2.422 (.122)	0.064 (.801)	3.141 (.085)	—	—	—	—	1.440 (.235)	0.717 (.400)
Typical antipsychotic use (yes/no), <i>F</i> ( <i>P</i> )	—	3.779 (.054)	0.629 (.430)	2.118 (.155)	—	—	—	—	2.323 (.133)	1.505 (.224)
Atypical antipsychotic use (yes/no), <i>F</i> ( <i>P</i> )	—	0.180 (.672)	0.045 (.832)	1.209 (.279)	—	—	—	—	0.091 (.765)	0.256 (.614)
Antidepressant use (yes/no), <i>F</i> / <i>T</i> ( <i>P</i> )	—	0.375 (.541)	1.229 (.270)	1.095 (.302)	-.0467 (.643)	—	-.0926 (.367)	0.157 (.876)	—	1.127 (.292)
Mood stabilizer use (yes/no), <i>F</i> ( <i>P</i> )	—	0.481 (.489)	0.655 (.420)	0.383 (.540)	—	—	—	—	—	0.599 (.411)
(v) Clinical symptoms										
PANSS total score, <i>R</i> ( <i>P</i> )	—	<b>.204 (.019)</b>	—	<b>.374 (.019)</b>	.030 (.857)	—	.081 (.783)	-.010 (.965)	<b>.279 (.038)</b>	.120 (.307)
PANSS positive score, <i>R</i> ( <i>P</i> )	—	.136 (.119)	—	.129 (.436)	-.021 (.902)	—	-.254 (.381)	-.013 (.952)	<b>.297 (.026)</b>	.000 (.999)
PANSS negative score, <i>R</i> ( <i>P</i> )	—	.166 (.057)	—	<b>.471 (.002)</b>	.070 (.678)	—	.179 (.541)	.007 (.975)	.167 (.218)	.148 (.208)
PANSS general score, <i>R</i> ( <i>P</i> )	—	<b>.208 (.017)</b>	—	.306 (.059)	.014 (.934)	—	.074 (.800)	-.019 (.930)	<b>.273 (.042)</b>	.131 (.268)



**Table 4.** (Continued)

Association Between BrainAGE and ...	Groups in Analysis 1					Groups in Analysis 2				
	HC <sub>1</sub>	SZ	MD	BPD	ARMS	HC <sub>2</sub>	ARMS-E	ARMS-L	RO-SZ	RE-SZ
SANS sum score, <i>R</i> ( <i>P</i> )	—	<b>.258 (.003)</b>	—	—	—	—	—	—	—	—
HAMD sum score, <i>R</i> ( <i>P</i> )	—	—	.086 (.398)	.195 (.228)	—	—	—	—	—	—

*Note:* BrainAGE, brain age gap estimation. Abbreviations are explained in the first footnote to tables 1 and 3. HC and ARMS: continuous/categorical variables were assessed using correlation analyses/*t* tests. Patients: continuous/categorical variables were tested using partial correlations/ANCOVAs, after correcting for age of onset and illness duration. *F*/*T*, *F* or *T* value in ANCOVA of Student *t* test; *R*, Pearson correlation coefficient. Bold and italicized values indicate significance at *P* < 0.05.

+5.5 [0.5], MD = +4.1 [0.6], BPD = +4.0 [1.1]; *F* = 2.0; *P* < .137). Effects were driven by early-onset MD (+6.7 [0.9]) and BPD (+6.9 [1.6]), which differed from the late-onset groups (MD: +2.8 [0.9], BPD: +1.8 [1.3]).

*BrainAGE Across Stages of SZ*

BrainAGE also varied across HC<sub>2</sub>, ARMS-E, ARMS-L, RO-SZ, and RE-SZ (*F* = 15.7; *P* < .001) groups, with increases in RE-SZ (+6.4 [5.6] y; *P* < .001), RO-SZ (+4.2 [6.4]; *P* < .001), and ARMS-L individuals (+2.7 [6.9]; *P* < .005) vs HCs (figure 1). Significant post hoc differences were found in the groups (1) RE-SZ vs RO-SZ (*P* < .034); ARMS-L (*P* < .001); and ARMS-E (*P* < .001), (2) RO-SZ vs ARMS-E (*P* < .001), and (3) ARMS-L vs ARMS-E (*P* < .005). A linear BrainAGE increase was detected from ARMS-E to RE-SZ (*R*<sup>2</sup> = .33; *T* = 5.3; *P* < .001), with the ARMS-E group showing negative BrainAGE effects. No main or interaction BrainAGE effects of disease stage (RO-SZ vs RE-SZ) and age of onset were found after controlling for PANSS total. However, the main BrainAGE effect of PANSS total survived after controlling for disease stage and age of onset (*F* = 4.4; *P* = .038).

*BrainAGE Associations With Sociodemographic and Clinical Parameters*

We did not observe any significant BrainAGE associations of psychotropic medications, nicotine, and alcohol in the patient (SZ, MD, and BPD) and ARMS groups (table 4) and no associations of sociodemographic parameters, nicotine/alcohol consumption, and different somatic conditions on BrainAGE in HCs (table 4; online supplementary analysis 1). A set of primarily negative and disorganized symptoms predicted BrainAGE in SZ subjects with *R*<sup>2</sup> = .26 (*T* = 6.5; *P* < .001; online supplementary analysis 2).

*Associations Between BrainAGE and the SVM Classification of Patient Status*

A cross-validated classification accuracy of 73.7% (AUC = 0.78) was observed in the SVM classification of 302 patients (SZ, MD, and BPD) vs 302 HCs (figure 2). Using BrainAGE as classifier in the same population, an accuracy of 65.7% (AUC = 0.71) was found at a cutoff value of +1.4 years. Classification accuracy for SZ patients vs HCs was higher both for the SVM (AUC = 0.81) and BrainAGE classifiers (AUC = 0.75). Average SVM decision and BrainAGE scores were highly correlated (*R*<sup>2</sup> = .53; *T* = 26.1; *P* < .001; figure 2). This correlation was due to a considerable overlap of age-predictive SVR patterns and brain regions involved in the SVM classification (figure 2).

**Discussion**

Studies recently employed MVPA methods to estimate age from structural MRI in large HC populations and

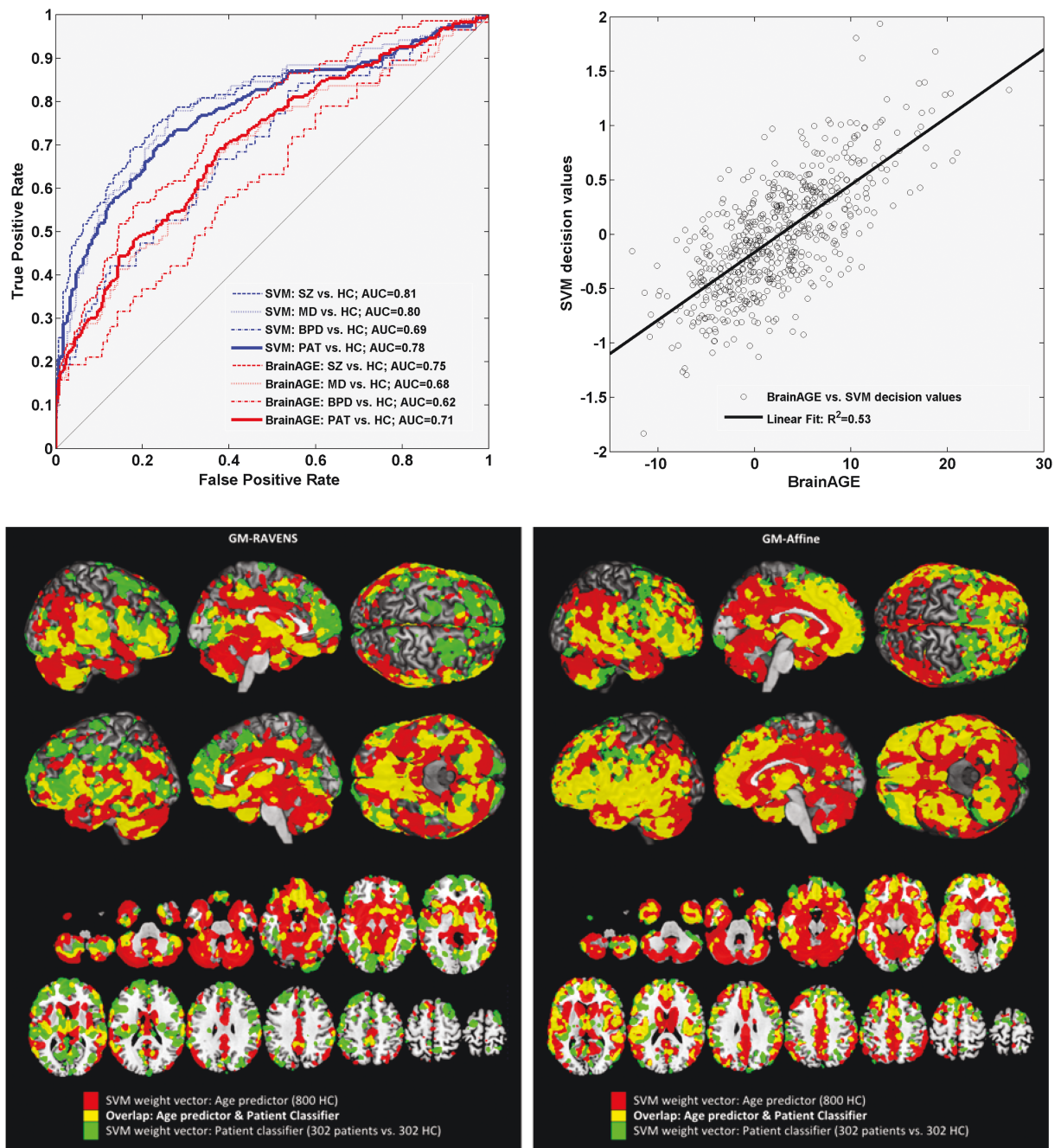


**Fig. 2.** Associations between support vector machines (SVM)-based age estimation and patient classification. Upper left: receiver operating characteristic analysis of (1) the SVM decision values of 302 patients (PAT) vs 302 healthy controls (HCs) (blue line) and (2) the respective brain age gap estimation (BrainAGE) scores (red line). Upper right: regression analysis of BrainAGE scores vs SVM decision values in the same population. Lower panel: qualitative characterization of the neuroanatomical overlap (yellow) between the SVM weight vectors of the age prediction system (red) and the patient classifier (green). In the gray matter (GM)-Regional Analysis of brain Volumes in Normalized Space condition (left), this overlap involved perisylvian, orbitofrontal, medial prefrontal, medial parietal cortices, and subcortical structures. In the affine GM condition, the extended overlap of age- and patient-predictive regions covered perisylvian, temporal, occipital, parietal, lateral and medial prefrontal, orbitofrontal and medial parietal, thalamic, and cerebellar regions.

reported very accurate prediction results across all ages and centers, with a minimum MAE of 1.1 years in children and adolescents.<sup>2-4</sup> Thus, age-related neuroanatomical variation seems to constitute a well-regulated intermediate phenotype of normal brain development

enabling individualized age inference. To our knowledge, our study is the first to demonstrate that this phenotype is commonly aberrant across major psychiatric diseases and the prodromal state of psychosis, suggesting “accelerated aging” effects already in early schizophrenic psychosis,

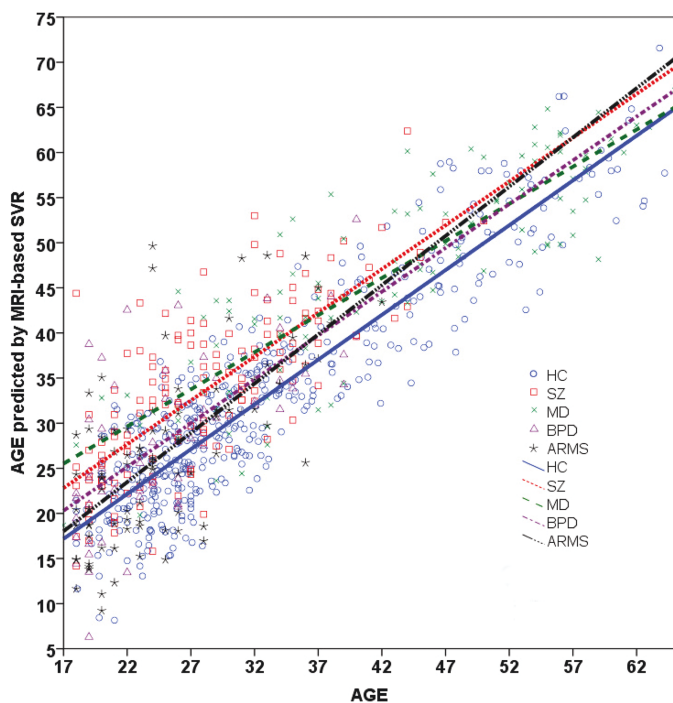


**Fig. 3.** Chronological age vs magnetic resonance imaging (MRI)-predicted age. Scatter plots and linear fits for chronological age vs MRI-predicted age in the HC, SZ, MD, BPD, and ARMS groups. ARMS, at-risk mental states; BPD, borderline personality disorder; HC, healthy control; MD, major depression; SZ, schizophrenia.

as well as in established MD and BPD. Moreover, these transnosological effects were more pronounced in early- vs late-onset MD and BPD, thus rendering these subgroups indistinguishable from schizophrenic patients. This aligns with the clinical observation of an earlier occurrence of both illnesses being associated with a more debilitating disease course, such as a higher incidence of suicidal attempts, prolonged duration of disease episodes as well as higher levels of psychiatric comorbidity.<sup>37–39</sup> Furthermore, our finding of increased BrainAGE in early-onset MD and BPD supports the hypothesis that the disruption of normal brain maturation during specific and critical time windows in adolescence and early adulthood constitutes a neurobiological predisposition for the development of psychopathological abnormalities across the affective and psychotic disease spectrums.<sup>1,7</sup>

Prospective MRI studies of normally developing individuals demonstrated a spatially and temporally asynchronous pattern of neuroanatomical brain maturation shifting from sensorimotor brain regions to higher order association cortices.<sup>12,40</sup> This process has been interpreted as a sequence of excitatory synaptic overelaboration followed by a reduction of excitatory and increase of inhibitory synaptic density.<sup>1</sup> This synaptic maturation is paralleled by ongoing white matter myelination, thus leading to a profound remodeling of neural networks, which optimizes neural connectivity through the exact temporal

coding of neural activity.<sup>41</sup> In this regard, recent neuroimaging studies of adolescent and adult schizophrenic patients suggested that the spatial pattern and intensity of neuroanatomical alterations in SZ may critically interact with the trajectory of maturational processes occurring in the normally developing brain: childhood-onset patients showed more pronounced neuroanatomical abnormalities in the sensorimotor and premotor cortices, whereas adult-onset patients were characterized by structural alterations in prefronto-temporo-limbic and subcortical brain regions.<sup>7,42</sup> Our study of adult patients extends these findings because our analyses revealed that (1) age- and disease-predictive GM variation overlapped within a prefronto-temporo-limbic pattern identified by recent meta-analyses of SZ studies (figure 2),<sup>13,43</sup> (2) an individual's deviation from the maturational reference trajectory considerably determined its likelihood of being classified as patient, particularly in SZ,<sup>44</sup> and (3) this signature of neuroanatomical dysmaturation was present across all diagnostic groups, correlating more with age of onset and symptom severity than with diagnosis. The latter finding agrees with previous studies revealing neuroanatomical patterns shared by affective and nonaffective psychoses,<sup>13</sup> as well as earlier disease onsets being paralleled by more pronounced brain abnormalities.<sup>7</sup> In this regard, our results may point to an age-dependent, transnosological domain of mental illness that may serve as a baseline for exploring more specific neuroanatomical biomarkers of different psychiatric phenotypes.

We did not observe significant associations between BrainAGE and illness duration in any of the patient groups, suggesting that BrainAGE does not capture progressive structural brain changes previously reported in severe mental disorders.<sup>9</sup> The finding of a linear BrainAGE increase from ARMS to RE-SZ individuals (figure 1) rather suggests that BrainAGE represents a neuroanatomical *vulnerability marker*, whose expression parallels the accumulating risk for adverse disease outcomes: risk for disease onset (ARMS-E: 7% transitions, ARMS-L: 57% transitions over 4 y) and risk for relapsing disease in RE-SZ vs RO-SZ patients. It is of note that the ARMS-E group showed a “decelerated brain aging” effect, which might be interpreted as a compensatory neural mechanism or maturational delay, as suggested by Douaud et al.<sup>42</sup>

However, due to the cross-sectional design of our study, these observations do not negate progressive structural brain alterations in the course of SZ and other psychiatric disorders. Progressive neuroanatomical abnormalities occurring after disease onset have been repeatedly reported by longitudinal studies<sup>9</sup> and have been linked to illness duration and antipsychotic treatment.<sup>45</sup> A likely interpretation of the nonsignificant associations between BrainAGE and these clinical variables (table 4; online supplementary analysis 2) may be that our multivariate age predictor spanned a

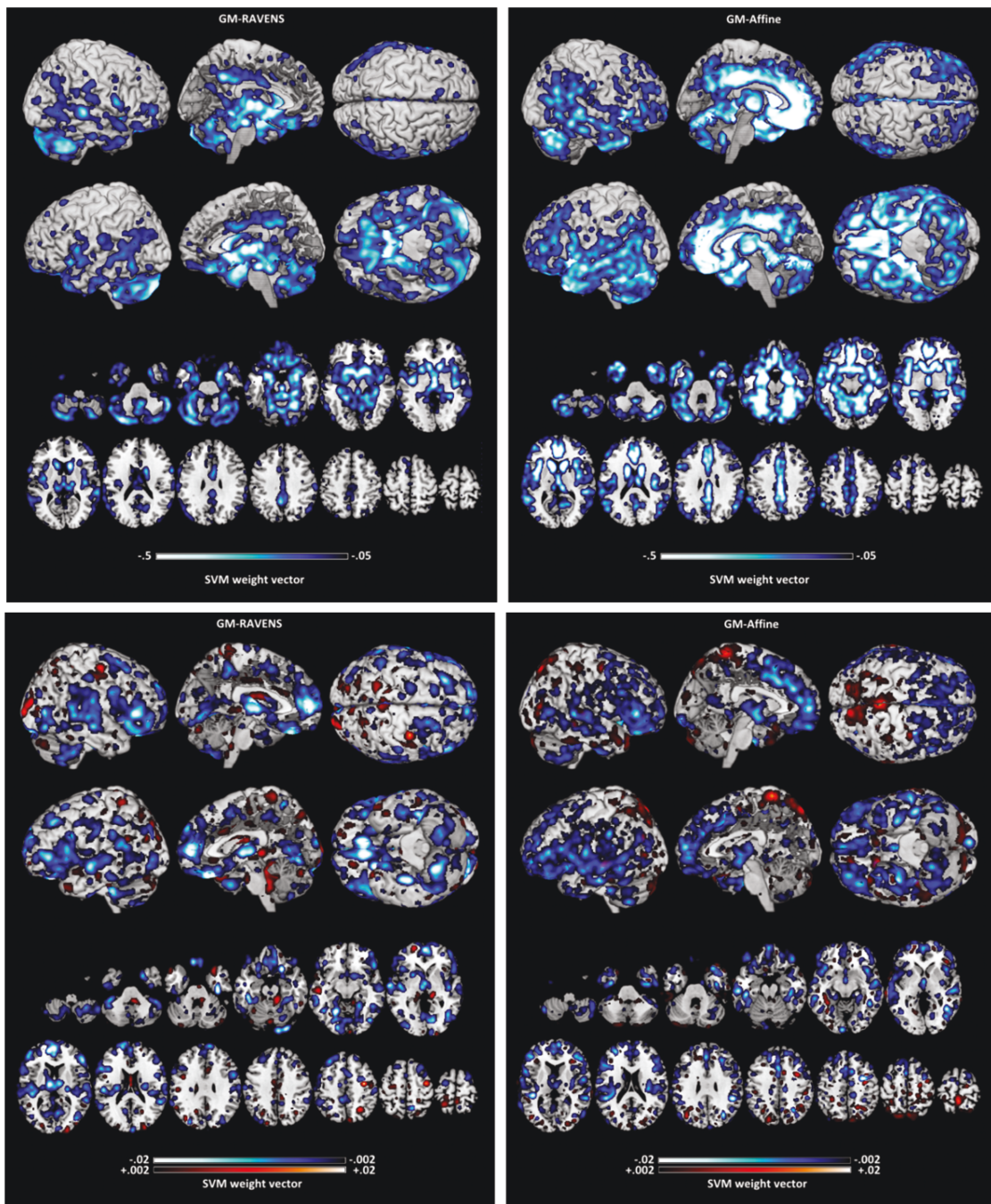


**Fig. 4.** Predictive patterns of support vector machines (SVM)-based age estimation and patient classification. Voxel relevance for age prediction (upper panels) and patient vs healthy control (HC) classification (lower panels) was visualized for the gray matter-Regional Analysis of brain Volumes in Normalized Space (GM-RAVENS; left) and the affinely registered GM data (right) (see online [supplementary methods 3](#)). Higher absolute voxel weights indicate greater voxel relevance for age prediction or patient classification. Age-predictive voxels in the GM-RAVENS condition mapped to subcortical and periventricular, orbitofrontal, cerebellar, limbic, and perisylvian regions, whereas a more extended age-predictive pattern involving cingulate, orbitofrontal, perisylvian, subcortical, and (para) limbic structures was found in the affine GM condition. Negative weights (cool colors) indicate the inverse relationship between age and GM volume/density. In the lower panels, negative voxel weights show patterns of GM volume or density reductions in 302 patients vs 302 HCs. In voxels with positive weights (warm colors), these relationships are reversed.

“neuroanatomical subspace” showing selective sensitivity for deviations from the normal maturational brain trajectory. Based on this hypothesis, it can be expected that clinical phenotypes with a possible neurodevelopmental

loading, such as “early vs late onset” and “deficit vs nondeficit outcome” particularly interfere with a neuroanatomical signature of accelerated brain aging. First, this hypothesis may be supported by our clinical SVR

analysis, which showed that 25% of BrainAGE variance in 125 SZ patients was primarily explained by negative and disorganization symptoms. This aligns with previous studies linking these symptoms to neuroanatomical abnormalities,<sup>46,47</sup> cognitive deficits, and poor social functioning,<sup>48</sup> together forming a “syndrome of accelerated aging” in SZ.<sup>11</sup> Second, BrainAGE increases were already detectable in antipsychotic-naïve ARMS-L individuals (+2.7 y). Because the illness duration in the RO-SZ patients was only 3.6 months and BrainAGE already measured was +4.2 years, an obvious interpretation may be that BrainAGE increases rapidly aggravate from attenuated psychosis to the established illness, in line with the hypothesis of a “late neurodevelopmental disturbance.”<sup>1,5</sup>

Finally, in none of the patient groups we did detect correlations between BrainAGE and alcohol, nicotine, or psychotropic medications, including antipsychotics, antidepressants, and mood stabilizers (table 4). Furthermore, we did not find significant effects of alcohol, smoking, educational, marital and occupational status as well as of major somatic conditions on BrainAGE in HCs (online supplementary analysis 1). These negative findings may further support a selective sensitivity of BrainAGE for abnormal neurodevelopment in severe mental illness. In summary, our results suggest that the BrainAGE framework provides a transnosological biomarker that (1) results from a disruption of normal brain maturation shared by different psychiatric phenotypes, (2) determines the case-by-case diagnostic performance of MRI-based disease classifiers, and (3) quantifies the risk for unfavorable clinical outcomes. Future investigations should thoroughly reevaluate the trait vs state nature of BrainAGE abnormalities and their specificity for neurodevelopmentally mediated mental illnesses by linking BrainAGE dynamics to the clinical, neurocognitive, and genetic dimensions of psychiatric disorders.<sup>49,50</sup>

### Supplementary Material

Supplementary material is available at <http://schizophreniabulletin.oxfordjournals.org>.

### Funding

Bundesministerium für Bildung und Forschung (German Ministry for Education and Science) (01EV0709 to C.G.); Open Access of Imaging Studies project (P50 AG05681, P01 AG03991, R01 AG021910, P50 MH071616, U24 RR021382, R01 MH56584).

### Acknowledgment

The authors have declared that there are no conflicts of interest in relation to the subject of this study.

### References

- Rapoport JL, Giedd JN, Gogtay N. Neurodevelopmental model of schizophrenia: update 2012. *Mol Psychiatry*. 2012;17:1228–1238.
- Brown TT, Kuperman JM, Chung Y, et al Neuroanatomical assessment of biological maturity. *Curr Biol*. 2012;22:1693–1698.
- Franke K, Luders E, May A, Wilke M, Gaser C. Brain maturation: predicting individual BrainAGE in children and adolescents using structural MRI. *Neuroimage*. 2012;63:1305–1312.
- Franke K, Ziegler G, Klöppel S, Gaser C; Alzheimer's Disease Neuroimaging Initiative. Estimating the age of healthy subjects from T1-weighted MRI scans using kernel methods: exploring the influence of various parameters. *Neuroimage*. 2010;50:883–892.
- Pantelis C, Yücel M, Wood SJ, et al Structural brain imaging evidence for multiple pathological processes at different stages of brain development in schizophrenia. *Schizophr Bull*. 2005;31:672–696.
- Rapoport JL, Gogtay N. Brain neuroplasticity in healthy, hyperactive and psychotic children: insights from neuroimaging. *Neuropsychopharmacology*. 2008;33:181–197.
- Gogtay N, Vyas NS, Testa R, Wood SJ, Pantelis C. Age of onset of schizophrenia: perspectives from structural neuroimaging studies. *Schizophr Bull*. 2011;37:504–513.
- Pantelis C, Yücel M, Wood SJ, McGorry PD, Velakoulis D. Early and late neurodevelopmental disturbances in schizophrenia and their functional consequences. *Aust N Z J Psychiatry*. 2003;37:399–406.
- Olabi B, Ellison-Wright I, McIntosh AM, Wood SJ, Bullmore E, Lawrie SM. Are there progressive brain changes in schizophrenia? A meta-analysis of structural magnetic resonance imaging studies. *Biol Psychiatry*. 2011;70:88–96.
- Kochunov P, Glahn DC, Rowland LM, et al Testing the hypothesis of accelerated cerebral white matter aging in schizophrenia and major depression. *Biol Psychiatry*. 2013;73:482–491.
- Kirkpatrick B, Messias E, Harvey PD, Fernandez-Egea E, Bowie CR. Is schizophrenia a syndrome of accelerated aging? *Schizophr Bull*. 2008;34:1024–1032.
- Giedd JN, Blumenthal J, Jeffries NO, et al Brain development during childhood and adolescence: a longitudinal MRI study. *Nat Neurosci*. 1999;2:861–863.
- Ellison-Wright I, Bullmore E. Anatomy of bipolar disorder and schizophrenia: a meta-analysis. *Schizophr Res*. 2010;117:1–12.
- Orrù G, Pettersson-Yeo W, Marquand AF, Sartori G, Mechelli A. Using Support Vector Machine to identify imaging biomarkers of neurological and psychiatric disease: a critical review. *Neurosci Biobehav Rev*. 2012;36:1140–1152.
- Pantelis C, Yücel M, Bora E, et al Neurobiological markers of illness onset in psychosis and schizophrenia: the search for a moving target. *Neuropsychol Rev*. 2009;19:385–398.
- Marcus DS, Wang TH, Parker J, Csernansky JG, Morris JC, Buckner RL. Open Access Series of Imaging Studies (OASIS): cross-sectional MRI data in young, middle aged, nondemented, and demented older adults. *J Cogn Neurosci*. 2007;19:1498–1507.
- Klosterkötter J, Hellmich M, Steinmeyer EM, Schultze-Lutter F. Diagnosing schizophrenia in the initial prodromal phase. *Arch Gen Psychiatry*. 2001;58:158–164.
- Koutsouleris N, Meisenzahl EM, Davatzikos C, et al Use of neuroanatomical pattern classification to identify subjects in

- at-risk mental states of psychosis and predict disease transition. *Arch Gen Psychiatry*. 2009;66:700–712.
19. Yung AR, Phillips LJ, McGorry PD, et al Prediction of psychosis. A step towards indicated prevention of schizophrenia. *Br J Psychiatry Suppl*. 1998;172:14–20.
  20. Borgwardt S, Koutsouleris N, Aston J, et al Distinguishing prodromal from first-episode psychosis using neuroanatomical single-subject pattern recognition. *Schizophr Bull*. 2013;39:1105–1114.
  21. Kay SR, Fiszbein A, Opler LA. The positive and negative syndrome scale (PANSS) for schizophrenia. *Schizophr Bull*. 1987;13:261–276.
  22. Andreasen NC. The Scale for the Assessment of Negative Symptoms (SANS): conceptual and theoretical foundations. *Br J Psychiatry Suppl*. 1989;7:49–58.
  23. Hamilton M. Development of a rating scale for primary depressive illness. *Br J Soc Clin Psychol*. 1967;6:278–296.
  24. Lambert M, Moritz S, Naber D. Pharmakotherapie der schizophrenie. In: Naber D, Lambert M, eds. *Schizophrenie*. Stuttgart, Germany: Georg Thieme Verlag; 2004:69–106.
  25. Riecher-Rössler A, Pflueger MO, Aston J, et al Efficacy of using cognitive status in predicting psychosis: a 7-year follow-up. *Biol Psychiatry*. 2009;66:1023–1030.
  26. Lieberman J, Chakos M, Wu H, et al Longitudinal study of brain morphology in first episode schizophrenia. *Biol Psychiatry*. 2001;49:487–499.
  27. Gaser C. Voxel-Based Morphometry Toolbox, version 8 (VBM8). 2009. <http://dbm.neuro.uni-jena.de>. Accessed October 3, 2013.
  28. Koutsouleris N, Patschurek-Kliche K, Scheuerecker J, et al Neuroanatomical correlates of executive dysfunction in the at-risk mental state for psychosis. *Schizophr Res*. 2010;123:160–174.
  29. Ou Y, Sotiras A, Paragios N, Davatzikos C. DRAMMS: deformable registration via attribute matching and mutual-saliency weighting. *Med Image Anal*. 2011;15:622–639.
  30. Davatzikos C, Genc A, Xu D, Resnick SM. Voxel-based morphometry using the RAVENS maps: methods and validation using simulated longitudinal atrophy. *Neuroimage*. 2001;14:1361–1369.
  31. Noble WS. What is a support vector machine? *Nat Biotechnol*. 2006;24:1565–1567.
  32. Schölkopf B, Smola A. *Learning with Kernels. Support Vector Machines, Regularization, Optimization and Beyond*. Cambridge, MA: MIT; 2002.
  33. Filzmoser P, Liebmann B, Varmuza K. Repeated double cross validation. *J Chemometrics*. 2009;23:160–171.
  34. Koutsouleris N, Borgwardt S, Meisenzahl EM, Bottlender R, Möller HJ, Riecher-Rössler A. Disease prediction in the at-risk mental state for psychosis using neuroanatomical biomarkers: results from the FePsy study. *Schizophr Bull*. 2012;38:1234–1246.
  35. Koutsouleris N, Gaser C, Bottlender R, et al Use of neuroanatomical pattern regression to predict the structural brain dynamics of vulnerability and transition to psychosis. *Schizophr Res*. 2010;123:175–187.
  36. Navot A, Shpigelman L, Tishby N, Vaadia E. Nearest neighbor based feature selection for regression and its application to neural activity. In: Weiss Y, Schölkopf B, Plattet J, eds. *Advances in Neural Information Processing Systems 18*. MIT Press: Cambridge, MA; 2006: 995–1002.
  37. Fava M, Alpert JE, Borus JS, Nierenberg AA, Pava JA, Rosenbaum JF. Patterns of personality disorder comorbidity in early-onset versus late-onset major depression. *Am J Psychiatry*. 1996;153:1308–1312.
  38. Korten NC, Comijs HC, Lamers F, Penninx BW. Early and late onset depression in young and middle aged adults: differential symptomatology, characteristics and risk factors? *J Affect Disord*. 2012;138:259–267.
  39. Zisook S, Rush AJ, Alcala A, et al Factors that differentiate early vs. later onset of major depression disorder. *Psychiatry Res*. 2004;129:127–140.
  40. Gogtay N, Sporn A, Clasen LS, et al Comparison of progressive cortical gray matter loss in childhood-onset schizophrenia with that in childhood-onset atypical psychoses. *Arch Gen Psychiatry*. 2004;61:17–22.
  41. Uhlhaas PJ, Singer W. The development of neural synchrony and large-scale cortical networks during adolescence: relevance for the pathophysiology of schizophrenia and neurodevelopmental hypothesis. *Schizophr Bull*. 2011;37:514–523.
  42. Douaud G, Mackay C, Andersson J, et al Schizophrenia delays and alters maturation of the brain in adolescence. *Brain*. 2009;132:2437–2448.
  43. Honea R, Crow TJ, Passingham D, Mackay CE. Regional deficits in brain volume in schizophrenia: a meta-analysis of voxel-based morphometry studies. *Am J Psychiatry*. 2005;162:2233–2245.
  44. Davatzikos C, Shen D, Gur RC, et al Whole-brain morphometric study of schizophrenia revealing a spatially complex set of focal abnormalities. *Arch Gen Psychiatry*. 2005;62:1218–1227.
  45. Smieskova R, Fusar-Poli P, Allen P, et al The effects of antipsychotics on the brain: what have we learnt from structural imaging of schizophrenia?—a systematic review. *Curr Pharm Des*. 2009;15:2535–2549.
  46. Koutsouleris N, Gaser C, Jäger M, et al Structural correlates of psychopathological symptom dimensions in schizophrenia: a voxel-based morphometric study. *Neuroimage*. 2008;39:1600–1612.
  47. Molina V, Hernández JA, Sanz J, et al Subcortical and cortical gray matter differences between Kraepelinian and non-Kraepelinian schizophrenia patients identified using voxel-based morphometry. *Psychiatry Res*. 2010;184:16–22.
  48. Lang FU, Kösters M, Lang S, Becker T, Jäger M. Psychopathological long-term outcome of schizophrenia – a review. *Acta Psychiatr Scand*. 2013;127:173–182.
  49. Fusar-Poli P, Borgwardt S, Bechdolf A, et al The psychosis high-risk state: a comprehensive state-of-the-art review. *Arch Gen Psychiatry*. 2012;70:1–14.
  50. Meyer-Lindenberg A. From maps to mechanisms through neuroimaging of schizophrenia. *Nature*. 2010;468:194–202.